https://doi.org/10.5194/egusphere-2025-1677
Preprint. Discussion started: 15 April 2025

Tracing near-surface runoff in a pre-Alpine headwater catchment

Anna Leuteritz[1*], Victor A. Gauthier[1*], Ilja van Meerveld[1]

[1]Department of Geography, Zurich University, Zurich, Switzerland

* joined first authorship

Correspondence to: V.A. Gauthier (victor.gauthier@lilo.org) and A. Leuteritz (anna.leuteritz@geo.uzh.ch)

Abstract. Near-surface flow pathways (i.e. overland flow and topsoil interflow) play a crucial role in runoff generation and solute transport in steep and humid catchments with low-permeability gleysols but remain understudied. We conducted sprinkling experiments on two large (>80 m^2) trenched runoff plots in the Swiss pre-Alps. One plot was located in a natural clearing in an open mixed forest and the other in a grassland. After reaching steady state conditions, we applied uranine and NaCl to the surface as line tracers, injected NaBr into the subsurface (at ~20 cm depth), and added deuterium-enriched water via the sprinklers to assess the particle velocities of near-surface flow pathways and the interaction between overland flow and topsoil interflow. We compare the velocities with the celerity, which was determined by temporarily adding more water to the plots at different distances (2, 4 and 6 m) from the runoff collectors. To trace overland flow and determine its flow path lengths, we applied brilliant blue dye at different locations on the surface of the plots.

The breakthrough curves highlighted the rapid transport of water and solutes. The average (over all tracer applications) of the maximum velocities for overland flow and topsoil interflow were 51 m h^{-1} and 30 m h^{-1} for the plot in the clearing, and 24 m h^{-1} and 17 m h^{-1} for the plot in the grassland, respectively. The tracer breakthrough curves highlight the interaction between overland flow and topsoil interflow as the NaBr that was injected in the subsurface in the clearing mainly exited the plot via overland flow. The celerity was 2-3 times higher than the velocity for overland flow for both locations and for topsoil interflow in the grassland plot. The celerity and velocity for topsoil interflow in the clearing were relatively similar, which we attribute to the importance of flow through large macropores. The overland flow pathways were relatively short for most locations (< 5 m) and confirmed the considerable interaction between overland flow and topsoil interflow as the dye often resurfaced a few meters below the initial infiltration points. Together, these results highlight the interaction between overland flow and topsoil interflow and the important role of macropores and soil pipes (particularly in forested areas) in rapidly transporting water and solutes from the steep, vegetated hillslopes to the streams.

https://doi.org/10.5194/egusphere-2025-1677
Preprint. Discussion started: 15 April 2025

1 Introduction

Hillslope trench studies (e.g., Freer et al., 1997; Woods and Rowe, 1996), sprinkling experiments and tracer experiments (Buttle and McDonald, 2002; Meißl et al., 2021; Montgomery et al., 1997) have been used to investigate hillslope flow pathways in different environments. They have shown that subsurface flow can rapidly transport water and solutes downslope (e.g., Anderson et al., 1997; Feyen et al., 1999; Graham et al., 2010; Jackson et al., 2016; Tsuboyama et al., 1994; van Verseveld et al., 2017; Weiler et al., 1999; Wienhöfer et al., 2009) and that preferential flow pathways can deliver a considerable fraction of the total subsurface flow (e.g., Anderson et al., 2009a; Ehrhardt et al., 2022; Noguchi et al., 1999; Uchida et al., 2005; Vlček et al., 2017). Experiments with dye tracers have highlighted that even though individual macropores are short, they form long connected networks of preferential flow pathways (Noguchi et al., 1999; Sidle et al., 2000, 2001). In well drained hillslopes, subsurface flow often occurs at the soil-bedrock interface (e.g., Freer et al., 2002; Tani, 1997; Tromp-van Meerveld and McDonnell, 2006; Weiler et al., 2006), but in catchments with lower permeability soils, flow through the biomat (Sidle et al., 2007), the O-horizon (e.g., Brown et al., 1999) and more permeable topsoil (e.g., Schneider et al., 2014) may be the most important pathway for lateral flow.

In pre-Alpine and Alpine catchments, overland flow (OF) may be an important runoff generation mechanism during large or intense events (Meißl et al., 2023; Scherrer et al., 2007; Weiler et al., 1999). However, for undisturbed vegetated hillslopes it is generally not widespread. Instead, OF tends to infiltrate into the soil after flowing over the surface for a short distance but only very few studies have actually studied the length of OF pathways in natural environments with tracers (Gerke et al., 2015; Maier et al., 2023) or based on temperature (Wolstenholme et al., 2020). Therefore, it is not clear how far OF travels over vegetated hillslopes and whether the water that infiltrates, mixes with the soil water or flows through preferential flow pathways further downslopes and then exfiltrates as return flow (RF; Dunne, 1978). Preferential flow pathways can be a major contributor to OF (Jones, 2010; Putty and Prasad, 2000). A few studies have shown that flow from preferential flow pathways consists mainly of water that was already stored in the soil (i.e., old water) (e.g., Bazemore et al., 1994; McDonnell, 1990) rather than precipitation, but it can contain some precipitation (i.e., new water) as well (Bachmair and Weiler, 2012; Kienzler and Naef, 2008; Klaus et al., 2013).

To understand hillslope runoff processes, it is important to distinguish the propagation of hydrological signals from the movement of the water itself (McDonnell and Beven, 2014). Celerity refers to the speed at which a hydrological response (e.g., a pressure wave) propagates through the system and determines the timing of the runoff responses. The particle velocity describes the travel time of water and solutes through a system. The celerity is generally (much) higher than the particle velocity, since pressure waves can be transferred rapidly through the system (e.g., Torres et al., 1998), while individual water particles require considerably more time to move downslope (McDonnell and Beven, 2014). Both, celerity and velocity depend on hydrological connectivity, flow pathways, moisture conditions and rainfall inputs (Hallema et al., 2016; McGuire and McDonnell, 2010; Saco and Kumar, 2004). So far there have been only a few combined studies on the celerity and velocity at the plot or hillslope scale (Rasmussen et al., 2000; Scaini et al., 2017; Torres et al., 1998; van Verseveld et al., 2017). These studies have shown that preferential flow pathways considerably influence the timing of surface flow responses and depend on vegetation (Bond et al., 2020; Monger et al., 2022). However, there is still a lack of field data about the celerity of near-surface flow pathways (Kienzler and Naef, 2008).

https://doi.org/10.5194/egusphere-2025-1677
Preprint. Discussion started: 15 April 2025

To better understand water and solute transport via near-surface flow pathways in humid catchments with low-permeability gleysols, we conducted sprinkling and tracer experiments on two trenched runoff plots (>80 m²) in the Swiss pre-Alps: one in a natural clearing in a mixed forest and the other on a grassland. Overland flow (OF) and subsurface flow through the topsoil with abundant roots (referred to as Topsoil Interflow, TIF) occur regularly (Gauthier et al., 2025). Macropores and soil pipes are common (Feyen et al., 1999; Schleppi et al., 2004; Schneider et al., 2014). Therefore, the velocity and celerity of OF and TIF were expected to be high. More specifically, we aimed to:

1. Quantify the celerity and velocity of overland flow (OF) and topsoil interflow (TIF)
2. Determine the interaction between OF and TIF
3. Assess the variability in OF pathway lengths

2 Study site

2.1 Studibach catchment

The study was conducted in the Studibach catchment, a 20-ha pre-Alpine headwater catchment located in the Alptal in Switzerland (47.038° N, 8.723°E). The elevation ranges from 1,270 to 1,650 m above sea level. The climate is humid, with an average annual precipitation of about 2,300 mm y^{-1}. Precipitation is evenly distributed throughout the year (Stähli et al., 2021) and snowfall accounts for about 30% of the annual precipitation (Stähli and Gustafsson, 2006). About a quarter of the annual precipitation is delivered by precipitation with a 10-minute intensity exceeding 6 mm h^{-1} (van Meerveld et al., 2018). The mean annual temperature is 5.7 °C (Stähli et al., 2021).

The topography is shaped by landslides and soil creep, with steep slopes (20-40°) and flatter areas. The latter are wetter and dominated by grasslands and wetland vegetation. The drier and steeper parts are covered by open coniferous forests (Hagedorn et al., 2000; Figure 1). The upper part of the catchment is used as a pasture during the summer months.

The gleysols are underlain by flysch, a heterogeneous calcareous and sedimentary bedrock with a low permeability (Mohn et al., 2000). The gleysols have a high silt and clay content (>85%), a low permeability (Schleppi et al., 1998), and an average depth of about 1 m, ranging from 0.5 m on the steep hillslopes and ridges to 2.5 m in flatter areas (van Meerveld et al., 2018; Rinderer et al., 2014). Flow through the more permeable topsoil (25 to 40 cm deep) is much faster due to the presence of macropores formed by roots and animal burrows (van Meerveld et al., 2018). The median (± standard deviation) of the saturated hydraulic conductivity of the surface, measured at eight locations in the lower part of the catchment using a 22 cm diameter double ring infiltrometer, was 76 ± 153 mm h^{-1} (Wadman, 2023).

Groundwater tables are typically close to the surface (Rinderer et al., 2014) and the catchment responds quickly to rainfall events, with streamflow increasing by several orders of magnitude within minutes to hours (van Meerveld et al., 2018). Rinderer et al. (2016) found that for about half of the analyzed events, streamflow at the catchment outlet began to rise earlier than the groundwater. This suggests that fast flow pathways play a key factor in the catchment's runoff dynamics.

https://doi.org/10.5194/egusphere-2025-1677
Preprint. Discussion started: 15 April 2025

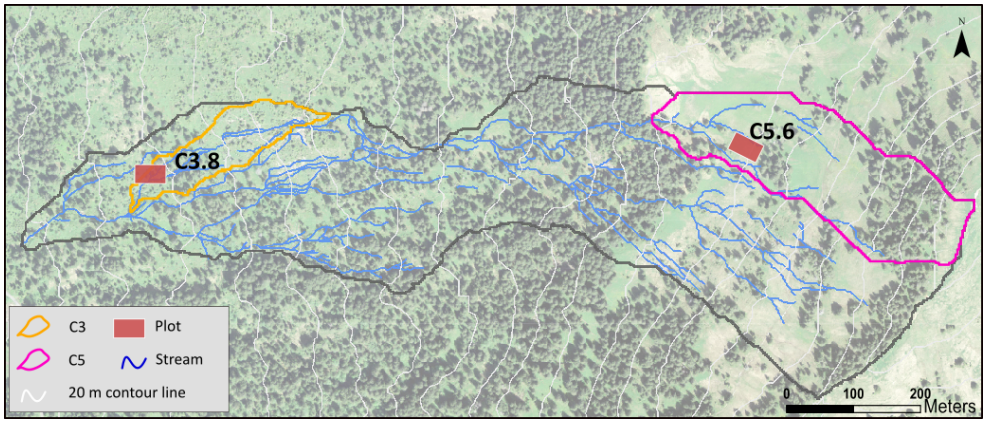

Figure 1: Map of the Studibach catchment (black) with the location of subcatchment C3 (orange outline) and C5 (pink outline), and the runoff plots where the sprinkling and tracer experiments were done (red rectangles, not to scale). One plot (C3.8) is located in a natural clearing in the forest, while the other (C5.6) is located in a grassland that is used as a pasture in summer. The gray lines represent the 20 m contour lines and the blue lines the mapped stream network. Background image: Swisstopo SwissImage (2023).

2.2 Plot locations

Two locations with relatively straight slopes, at least 15 m wide and 15 m long were selected for the sprinkling and tracer experiments (Figure 1; Table 1). One plot is located in a natural clearing in an open coniferous forest dominated by *Picea abies* (plot C3.8; Figure 2a) and the other (plot C5.6; Figure 2b) is located in a meadow that is used as a cattle pasture during the summer months. We refer to these plots as the clearing and grassland plot, respectively.

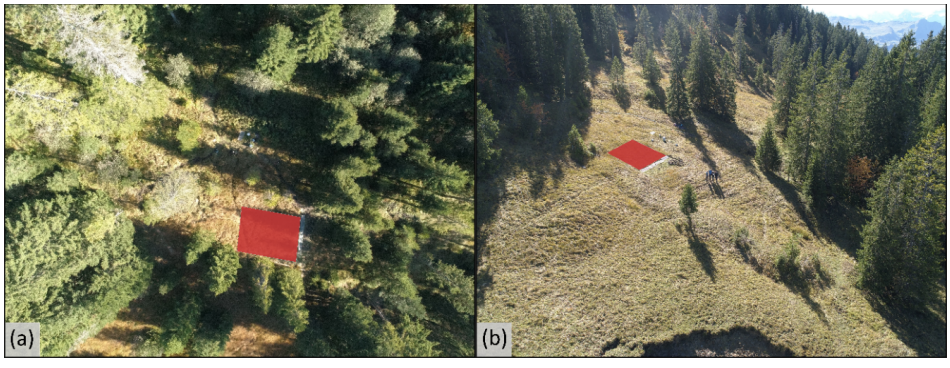

Figure 2: Drone images of the plots in (a) the natural clearing in the open forest and (b) the grassland area. The location of the runoff plot areas is highlighted by the red trapezoids. For the location of the plots in the catchment see Figure 1.

The vegetation on the plot in the natural clearing consists primarily of grasses, alpine flowers (*Chaerophyllum hirsutum*, *Lactuca virosa*, *Aconitum napellus*, and *Filipendula ulmaria*), and horsetails (*Equisetum* spp.). The mean

https://doi.org/10.5194/egusphere-2025-1677
Preprint. Discussion started: 15 April 2025

slope is 9°. The surface is hummocky and contains some depressions. The soil profile consists of a 10 cm organic rich horizon, a topsoil horizon that is rich in organic material up to 30 cm deep, and a dense, reduced clay with small stones (Ø <5 cm) that extends to at least 70 cm below the soil surface. The root density decreases with depth into the topsoil (Figure S1). The first 10 cm of soil contains many small roots and some big roots. There were many partially decomposed pieces of wood, such as old branches or small sections of trunk within the first 70 cm of soil. Most old roots were buried in the topsoil (up to 30 cm depth) and occasionally extended into the dense clay layer.

The vegetation of the grassland plot consists of horsetails (*Equisetum* spp.), small alpine flowers (*Succisa pratensis*, *Leontodon helveticus*, *Orchis mascula*), grasses, and scattered moss (*Selaginella helvetica*). The mean slope is 18°. The soil surface is more uniform than for the plot in the clearing. However, there were small "terraces and lobes", which could be attributed to solifluction processes or cattle trampling. The soil profile consists of an organic rich horizon up to 7 cm deep, a topsoil horizon, composed of clay and organic material extending to 25 cm below the soil surface, and a subsoil of reduced clay that extended to at least 75 cm. Root density was highest in the upper 7 cm of the soil and decreased in the topsoil. The roots were small (Ø <0.5 mm). There were only a few large pieces of half-decomposed wood throughout the soil profile.

Table 1: Overview of the plots and properties for the organic horizon (measured at 2-7 cm) and the topsoil (measured at 10-15 cm). The Topographic Wetness Index (TWI) is based on the calculations of (Rinderer et al., 2014) for a 6 m smoothed Digital Elevation Model. The slope was measured in the field. The porosity, moisture content at field capacity and drainable porosity are based on measurements for a soil core with the Hyprop (METER Group, USA). The organic matter content is based on the loss on ignition.

	Clearing		**Grassland**	
TWI	7.0		5.9	
Slope	9°		18°	
Soil depth	2-7 cm	10-15 cm	2-7 cm	10-15 cm
Soil bulk density (g cm^{-1})	0.21	0.23	0.53	0.38
Porosity (%)	85	84	80	79
Moisture content at field capacity (pF 1.8) (%)	68	65	70	73
Drainable porosity	17	19	11	6
Organic Matter content (%)	54	43	32	23

3 Methods

3.1 Runoff plots

3.1.1 Plot setup

At the lower end of the ~80 m^2 plots, an eight-meter-long trench was excavated perpendicularly to the slope, following the methodology of Maier and van Meerveld (2021) and Weiler et al. (1999). To collect the topsoil interflow (TIF), drain foil was placed along the trench face to block the lateral subsurface flow flowing through the topsoil. A drainage tube was wrapped in the foil and placed at the bottom of the 40 to 70 cm deep trench to

https://doi.org/10.5194/egusphere-2025-1677
Preprint. Discussion started: 15 April 2025

collect the water and route it to an Upwelling Bernoulli Tube (UBeTube). The trench was backfilled to ensure slope stability. An eight-meter-long gutter was installed on the surface and plastic foil was inserted into the soil (at ~3 cm depth on average) to guide the overland flow into the gutter. The water was then routed to another UBeTube via a hose. A fiberglass roof was installed over the gutter to prevent direct precipitation from entering the gutter.

The UBeTubes were built at the University of Zurich following the design of Stewart et al. (2015) using 10 cm diameter PVC pipe in which a v-notch was cut with water jet cutter (see Gauthier et al. (2025)). A small piece of hose was attached to the UBeTube, just below the V-notch to facilitate the collection of water and to direct it to two separate boxes in which the water quality sensors were installed (see section 3.2.3.2). A conductivity, temperature, and pressure logger (DCX-22-CTD, Keller Druck, Switzerland) was installed in each UBeTube. To determine the water level from the pressure measurements, a barometric logger (DCX-22, Keller Druck, Switzerland) was placed outside the UBeTubes. The barometric loggers were wrapped in a heat-reflecting foil to minimize temperature-related errors (Shannon et al., 2022). Laboratory-based rating curves were used to obtain the flow rate from the measured water levels.

At each runoff plot, we installed soil moisture sensors (TEROS 12 and GS3, METER Group, USA) at 5, 15 and 25 cm below the soil surface at 2.5, 5, and 7.5 m from the trench. The sensors were connected to ZL6 and EM50 data loggers (METER Group, USA) and recorded soil moisture at a 5-minute frequency.

3.1.2 Sprinkler set up and rainfall measurements

For the rainfall simulation, we used Senninger I-Wob sprinklers (nozzle number 22) installed along the centre line of the plot at 2.5 m above the ground surface (Figure 3). These sprinklers are known to provide water with a relatively uniform spatial distribution and a representative raindrop size distribution (Maier and van Meerveld, 2021; van Meerveld et al., 2014). For the experiments in the clearing, stream water was applied to the sprinklers at 3 m and 7.5 m upslope from the trench. The stream water was collected from a location upstream and routed directly to the sprinklers via garden hoses (i.e., gravity driven; ~100 m elevation difference). For the experiments on the grassland plot, there was limited flow from the headwater streams and water pressure was insufficient. Thus, for these experiments, we used a pump (MP2454, Dolmar, Germany). Because of this constraint, we only used one sprinkler, located 5 m from the trench (Figure 3).

At both plots, rainfall was recorded with two tipping bucket rain gauges (Davis Instruments Corp., USA with Odyssey data logger; Dataflow Systems, New Zealand; 0.2 mm resolution) installed at 4.0 m and 6.5 m from the trench (Figure 3). Additionally, we installed five rain collectors (funnel diameter: 100 mm) to determine the uniformity of the applied rainfall. The mean rainfall intensity was 24 mm h^{-1} for the experiments in the clearing and 39 mm h^{-1} for the experiments in the grassland (Table 2). These mean intensities correspond to intense rainfall events that occur one to two times per year based on 38 years of hourly precipitation data from the Erlenhöhe meteorological station, located 500 m from the Studibach outlet. Variations in mean intensity for the experiments in the clearing were attributed to small stones partially obstructing the water hose. For the experiments in the grassland, there were occasional issues with the pump or its power supply, leading to larger variations in the applied rainfall intensity.

https://doi.org/10.5194/egusphere-2025-1677
Preprint. Discussion started: 15 April 2025

3.2 Sprinkling experiments

3.2.1 Overview of the experiments

We conducted three different types of experiments on both plots: 1) water pulse experiments to determine the celerity, 2) tracer experiments to determine the velocity and mixing of OF and soil water, and 3) a blue-dye experiment to determine the length and shape of the OF pathways (Table 2). All experiments were conducted during steady state conditions, which were established by irrigating the plots until the OF and TIF rates were stable. There was a thin layer of snow (~5 cm) on the grassland plot prior to the first experiment. Some snow was carefully removed and the plot was irrigated until no visible snow patches remained on the surface (and the OF and TIF rates were stable). Due to the limited number of daylight hours and nighttime temperatures falling below 0°C, overnight sprinkling was not possible for the grassland plot (Table 2).

Table 2: Details of the different experiments for the plot in the natural clearing in the open forest and the plot in the grassland: date, sprinkling duration, and mean rainfall intensity ± standard deviation

Plot location and type of experiments	Date (dd.mm.yyy)	Duration of the experiment (h)	Mean intensity (mm h^{-1})
Clearing			
Water pulse experiments	08.08.2023	8	22 ± 2
Tracer experiments	09 and 10.08.2023	25	22 ± 2
Blue dye experiment	16.08.2023	4	28 ± 4
Grassland			
Water pulse experiments	09.11.2023	3.5	41 ± 5
Tracer experiments	08.11.2023	3.0	35 ± 13
Blue-dye experiment	09.11.2023	3.5	41 ± 5

3.2.2 Water pulse experiments

To determine the celerity of OF and TIF, we added additional water (~10 L min^{-1}) during the continued sprinkling across the plot at various distances from the trench (2, 4, and 6 meters) using an 8 m long hose with small holes (soaking hose) that was suspended across the plot at ~50 cm above the surface. This "water pulse" (in addition to the rainfall from the sprinklers) increased the OF and TIF rates at the bottom of the plots above the steady state flow rates. Once a response was visually observed, the supply of the additional water was interrupted and the system was allowed to return to the steady state flow rates.

3.2.3 Tracer experiments

3.2.3.1 Tracer application

After steady state was reached for both OF and TIF, NaCl and uranine were applied to the surface of the plots as line tracers, NaBr was added to the subsurface, and deuterium labelled water was added via the sprinklers, (Table 3; Figure 3). All tracers were applied in solution. More specifically, in the clearing, we applied two lines of NaCl and uranine (NaCl 1 and NaCl 2 and uranine 1 and uranine 2, respectively) by uniformly pouring the dissolved tracer across the plot within 1 minute (Table 3). The second line of NaCl and uranine tracer was applied 2.72 hours after the application of the first lines, well after the peak concentrations had passed according to manual

https://doi.org/10.5194/egusphere-2025-1677
Preprint. Discussion started: 15 April 2025

220 measurements of the Electrical Conductivity (EC) using a hand-held conductivity sensor (WTW Multi 3420, WTW Measurement Systems Inc). At the time of the first NaCl and uranine tracer application, we also applied 545 g NaBr to the subsurface via four 45 mm diameter PVC piezometers installed at 20 cm depth at 7.5 m from the trench. For the plot in the grassland, we applied only one line of NaCl and uranine to the surface and 1500 g of NaBr to the subsurface via five piezometers installed at 6 m from the trench (Figure 3).

225 For the experiment in the clearing, we filled two ~500 L containers with stream water and added 150 mL of 75% deuterium water, yielding a δ^2H of 1516‰. The sprinklers were connected to these containers (and thus sprinkled deuterium enriched water to the surface) for 30 min. For the grassland site, only one container was filled with stream water. The addition of 150 mL of 75% deuterium water, yielded a δ^2H of 2604‰. The sprinklers applied the deuterium enriched water to the surface of the grassland plot for 17 minutes.

230

Table 3: Details of tracer experiments on the plots in the natural clearing in the open forest and the plot in the grassland.

Tracer experiment location and employed tracers	Type of application	Distance from trench (m)	Applied tracer mass, volume of solution
Clearing			
NaCl 1	Line application	2.7	250 g; 4 L
NaCl 2	Line application	6.0	750 g; 4 L
Uranine 1	Line application	4.5	0.4 mL; 4 L
Uranine 2	Line application	7.5	0.4 mL; 4 L
NaBr	Subsurface injection	7.5	545 g; 2.25 L
D_2O-enriched water	Surface application	-	300 mL; ~1000 L
Grassland			
NaCl	Line application	2.7	250 g; 4 L
Uranine	Line application	4.5	0.4 mL; 4 L
NaBr	Subsurface injection	6.0	1500 g; 2.25 L
D_2O-enriched water	Surface application	-	150 mL; ~500 L

https://doi.org/10.5194/egusphere-2025-1677
Preprint. Discussion started: 15 April 2025

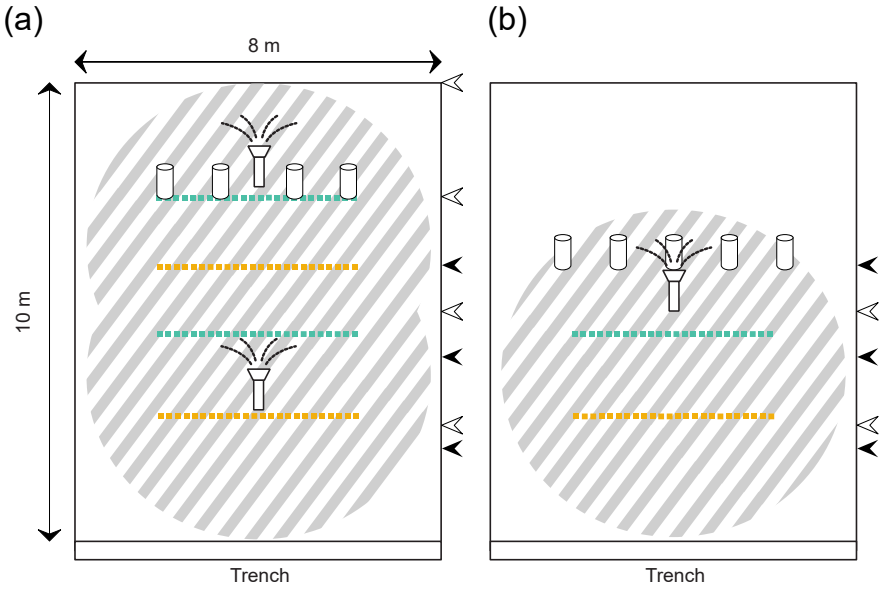

Figure 3: Schematic overview of the tracer applications for the plots in the natural clearing (a) and in the grassland (b). Deuterium-enriched water (striped pattern) was applied to the surface via the sprinklers. NaCl (yellow) and uranine (green) were applied as lines at varying distances from the trench. NaBr was applied to the subsurface at a depth of 20 cm via piezometers. The location of the lines of the water pulses (black arrow heads) and blue dye (white arrow heads) are indicated on the side of the plots. The locations of the sprinklers are indicated with the sprinkler icons.

3.2.3.2 Sample collection and water quality sensors

During the tracer experiments, we manually collected samples of OF and TIF. For the experiment in the clearing, samples were collected at a one-minute interval for the first 41 minutes after the first tracer application (NaCl 1, uranine 1, NaBr, and D_2O-labelled water), followed by sampling every two minutes for 24 minutes, and sampling every five-minutes for 90 minutes. After the second line tracer application (NaCl 2 and uranine 2), samples were again collected at a one-minute interval for 40 minutes, followed by a five-minute interval for an additional 150 minutes. We used automatic samplers (model no. 6712, Teledyne ISCO, USA) to collect OF and TIF samples overnight at a one-hour interval. However, only the automatic sampler for OF functioned. Therefore, we manually collected three additional TIF samples the next day at intervals of one to two hours. In the grassland, the sampling intervals ranged between one and two minutes following the tracer application and continued for 2.5 hours. In addition to the sampling of OF and TIF, we sampled the stream that fed the sprinklers (every 1-2 hours for the experiments in the clearing and every 30 minutes for the experiments in the grassland). All samples were collected in 25 ml glass vials without headspace, stored in a fridge at 4°C, and filtered (0.45 µm SimplepureTM syringe filter) within a few days after sampling.

We recorded the electrical conductivity (EC) of OF and TIF with a Multi 3420 conductivity sensor (WTW Measurement Systems Inc) while we took the samples, and automatically (every minute) using the loggers (DCX-22-CTD, Keller Druck, Switzerland) installed in the UBeTubes. The outflow from the UBeTubes went to sampling

https://doi.org/10.5194/egusphere-2025-1677
Preprint. Discussion started: 15 April 2025

boxes that were equipped with a fluorescence sensor (Cyclops-7F Submersible Sensors, Turner Design, USA, with a Cyclops-7 logger, PME, USA), set to a one-minute measurement interval and calibrated prior to the experiments.

3.2.3.3 Laboratory analyses

We analysed the selection of samples for bromide concentrations at the Physics of Environmental Systems laboratory at ETH Zurich (Switzerland) using ion chromatograph (861 Advanced Compact IC, Metrohm AG, Switzerland). Another selection of samples was analysed for the abundance of the stable isotopes of hydrogen and oxygen (from here on named stable water isotopes for brevity) using a cavity ring-down spectroscope (CRDS; L2140-i or L2130-i, Picarro, Inc., USA) at the Chair of Hydrology at the University of Freiburg, Germany. The analytical uncertainty is ± 0.6 ‰ for δ^2H.

3.2.3 Blue dye experiment

Brilliant blue dye was used to trace the OF pathways. As with the other experiments, rainfall was applied to the plots until steady state conditions were reached. The blue dye was manually applied along the surface of the plot as a line at 2.5, 5, 7.5, and 10 m from the trench in the clearing, and at 2.5 and 5 m from the trench in the grassland (Figure 3). For each line (~ 6 to 7-m-long), we used two 1.5 L bottles containing the 3 mg L^{-1} brilliant blue dye and applied it as uniformly as possible within a minute. Immediately following the dye application, the OF pathways were marked using tree types of flags: one indicating the flowpath from the application to where it infiltrated into the soil, another indicating exfiltration (i.e., reappearance) of the dye, and a last one marking the second re-infiltration. Once the flow pathways had all been marked, the pattern of the OF pathways was sketched in a notebook using a 25 cm grid and photographs were taken with a drone (Phantom II, DJI, China) to complement the manual sketches.

In the clearing, the tall grass was cut 7 days prior to the blue dye experiment (but after the water pulse and tracer experiments) to be able to observe the flow pathways. In the meadow, this was not necessary because the experiment took place in November when the vegetation was not as tall and it was able to see the ground surface.

3.3 Data analyses

3.3.1 Hydrometric responses

Flow rates were calculated from the water levels in the UBeTubes based on rating curves developed in the laboratory ($Q = \alpha h^{\beta}$, where $\alpha = 0.24 \pm 0.08$, $\beta = 1.88 \pm 0.27$, h is the water level above the bottom of the V-notch (in cm), and Q the flow rate (in L min^{-1})). The estimated uncertainty in the flow rate is 12% at low flow rates (<2 L min^{-1}) and 5% at higher flow rates. Runoff ratios were calculated by dividing the total amount of OF or TIF by the total rainfall. All analyses for the flow data were done in Python (version 3.12), using the packages *Pandas*, *Scipy*, *Matplotlib* and *Seaborn*.

3.3.2 Arrival times

The celerity and particle velocity were based on the timing of the first increase in the water level in the UBeTube and the first arrival of the tracer (i.e., timing of the sample with a concentration above background) after application, respectively. They are thus the maximum celerity and velocity. No adjustments were made for potential delays caused by the transfer through the drainage system or the gutter as these were assumed to be small. However, to determine the uncertainty of the celerity and velocity, we assumed an uncertainty in the timing of 2 minutes and uncertainty in the distance of 0.1 m.

https://doi.org/10.5194/egusphere-2025-1677
Preprint. Discussion started: 15 April 2025

3.3.3 Tracer recovery

One-minute time series of the bromide concentrations and δ^2H were generated by linear interpolation between the measurements. The background concentrations were subtracted from the measured concentrations after the tracer application to obtain the breakthrough curves. The background electrical conductivity (EC) and uranine concentrations for OF and TIF were based on the average of the measurements after steady state conditions were reached and 15 minutes before the first salt and uranine applications. Background concentrations of bromide were below the detection limit. A laboratory calibration was used to convert the EC minus the background to NaCl concentrations.

The recovered tracer mass was estimated by integrating the mass fluxes (concentration minus the background concentration multiplied by the flow rate). For the calculations of the tracer recovery, we assumed that the sprinklers did not apply any uranine or bromide as these concentrations were all below the detection limit. We, similarly, assume that the chemistry of the irrigation water had a negligible effect on the chemistry of OF and TIF, given that the plots were irrigated for several hours a day before the experiments and the EC in OF and TIF remained relatively stable during this time. Furthermore, the stream water that was used for sprinkling had a higher EC than OF and TIF after steady state conditions were established. We expected that the NaBr that was added to the subsurface would take considerably more time to reach the OF and TIF collection systems than the NaCl that was added to the surface at a downslope location, and that interference with the EC measurements would be minimal. However, the breakthrough of NaBr was quick as well (see results section 4.3). Still, the peak concentration of NaBr would have increased the EC by only 2 µS cm^{-1}. This is comparable to the 1 µS cm^{-1} resolution of the sensor and leads to an overestimation of the calculated NaCl concentrations by about 1 mg l^{-1}. We considered this overestimation acceptable considering all other uncertainties and thus did not correct the EC derived estimates of NaCl for the NaBr concentrations. Still collectively, these assumptions lead to some uncertainty in the recovery of the NaCl tracer.

We report the tracer recovery rates for the first 100 minutes to allow for a comparison between the two plots, as sampling for the grassland plot was limited to 100 minutes after tracer application. For the clearing, we additionally report the recovery until the time of the second line tracer application (NaCl 2 and uranine 2) and the end of the experiment (24 hours). The estimated uncertainty in the flow rates (see section 3.3.1) leads to a considerably larger uncertainty in the recovered mass than the uncertainty in measured tracer concentration. Thus, we did not consider the uncertainty in the concentrations in the uncertainty of the tracer recovery.

3.3.4 Two-component mixing model

We applied a two-component mixing model to estimate the fraction of the deuterium labelled water (f_e) in OF and TIF:

$$f_e = \frac{(C_S - C_{pe})}{(C_e - C_{pe})}$$

where C_S is the δ^2H for the OF or TIF sample, C_{pe} is the δ^2H of the OF and TIF prior to the application of the labelled water (mean of -65.45 ‰ and -64.93 ‰ for OF and TIF for the experiment in the clearing and -77.16 ‰ and -78.8 ‰ for OF and TIF for the experiment in the grassland, respectively), and C_e is the δ^2H for the labelled sprinkler water (1516 ‰ and 2604 ‰ for the experiments in the clearing and grassland, respectively). Note that due to the considerable amount of water applied to the plots to test the sprinklers, reach steady state conditions,

https://doi.org/10.5194/egusphere-2025-1677
Preprint. Discussion started: 15 April 2025

and for the clearing also the water pulse experiments, the δ^2H of the OF or TIF samples collected right before the application of the labelled water were similar to those of the applied unlabelled water (-67.7‰ for the plot in the clearing and -73.1‰ for the grassland plot).

4. Results

4.1 Overall response of the plots to the sprinkling

In the clearing, steady state conditions were reached after on average 35 minutes of sprinkling for OF and 51 minutes for TIF. Soil moisture increased on average (for the three locations in each plot) by 10% at 5 cm, 1% at 15 cm and 5% at 25 cm during this time. The flow rate during the steady state conditions was almost twice as high for TIF than OF (Figure 4a), with runoff ratios during the steady state conditions of ~ 20% for OF and ~ 46% for TIF. During the water pulse experiments, the OF and TIF flow rates were relatively constant, except during and following the application of the water pulses (Figure 5). During the tracer experiment, the flow rate was constant for OF, but for TIF there was a 25% increase between 375 and 500 minutes. As there was no change in the sprinkling intensity, we think that this increase is mainly caused by changes in the boundary conditions, particularly on the right side of the plot (looking upslope) where a long surface flowpath was observed during the blue dye experiments (see section 4.4). As we walked along this side of the plot and the soil on this side of the plot became very muddy, we may have influenced this flow pathway (e.g., temporarily blocked part of it).

For the grassland plot, steady state conditions were reached after on average 30 minutes of sprinkling for OF and 26 minutes for TIF. Soil moisture content increased minimally during this time. The OF rate was much larger for OF than TIF, with runoff ratios of 44% and 5%, respectively (Figure 4b). Because of the use of the pump and occasional issues with the power supply (e.g., to refill the petrol), the rainfall rate (Table 2) and flow rates fluctuated more than for the experiments in the clearing. There was a decline in the precipitation intensity and flow rates at 90 and 140 minutes after switching the source of the sprinklers for the tracer experiments (Figure 4b) and at 20 and 135 minutes during the water pulse experiment (Figure 5).

https://doi.org/10.5194/egusphere-2025-1677
Preprint. Discussion started: 15 April 2025

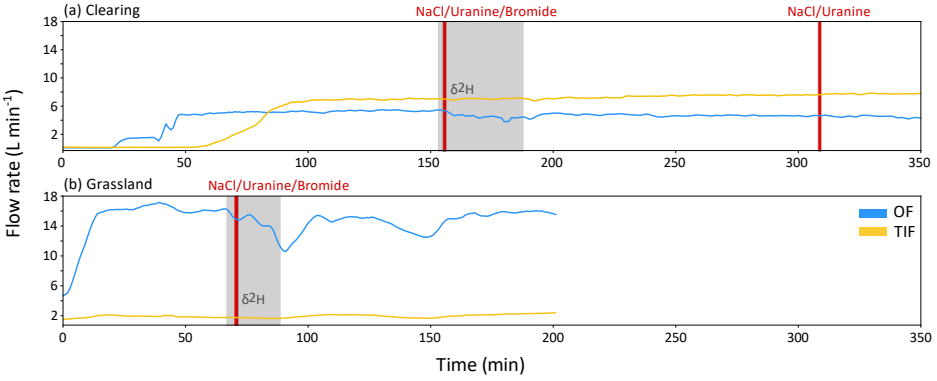

Figure 4: Time series of the OF (blue) and TIF (orange) flow rates (L min^{-1}) during the tracer experiments on the plot in the clearing (a) and the plot in the grassland (b). The period when deuterium-enriched water was applied is indicated by the grey shading. The times of the NaCl, uranine and bromide tracer applications are indicated by the vertical red lines.

4.2 Water pulse experiments

In the clearing, the water pulses at 2 m and 4 m from the trench produced a clear response for OF and TIF. The response was less pronounced for the pulse applied at 6 m from the trench (Figure 5a). Water was also applied at 8 m, but did not lead to a measurable response (data not shown). The increase in the flow above the steady state flow rate was more than four times larger for TIF than OF (Figure 5a). The calculated celerities were higher and more variable (depending on the distance from the trench) for OF (mean ± standard deviation: 150 ± 80 m h^{-1}) than for TIF (34 ± 5 m h^{-1}), in part due to the very high celerity (240 m h^{-1}) for the water pulse applied at 4 m from the trench (Table 4). The celerity for OF was on average of a factor 4 times (range: 2.8-8.0) higher than for TIF. The use of the ± 2 minutes uncertainty for the first response (2 measurements) was similar to the response time, leading to very high uncertainties for the celerity of OF (Table 4).

In the grassland, all three water pulses (at 2 m, 4 m and 6 m) produced a clear flow response. In contrast to the results for the plot in the clearing, the increase in OF due to the water pulse was much larger than for TIF (Figure 5b). The mean value for the celerity for OF (64 ± 7 m h^{-1}) and TIF (41 ± 10 m h^{-1}) were more similar for the three application distances than for the experiments in the clearing (Table 5). The celerity for OF was on average almost a factor two (range: 1.3-2.0) higher than for TIF. The celerity for OF in the grassland was almost two times smaller for the grassland than for the clearing (when excluding the high celerity for the experiment at 4 m in the clearing). The celerities for TIF were more similar, though somewhat higher in the grassland than the clearing (Table 4).

https://doi.org/10.5194/egusphere-2025-1677
Preprint. Discussion started: 15 April 2025

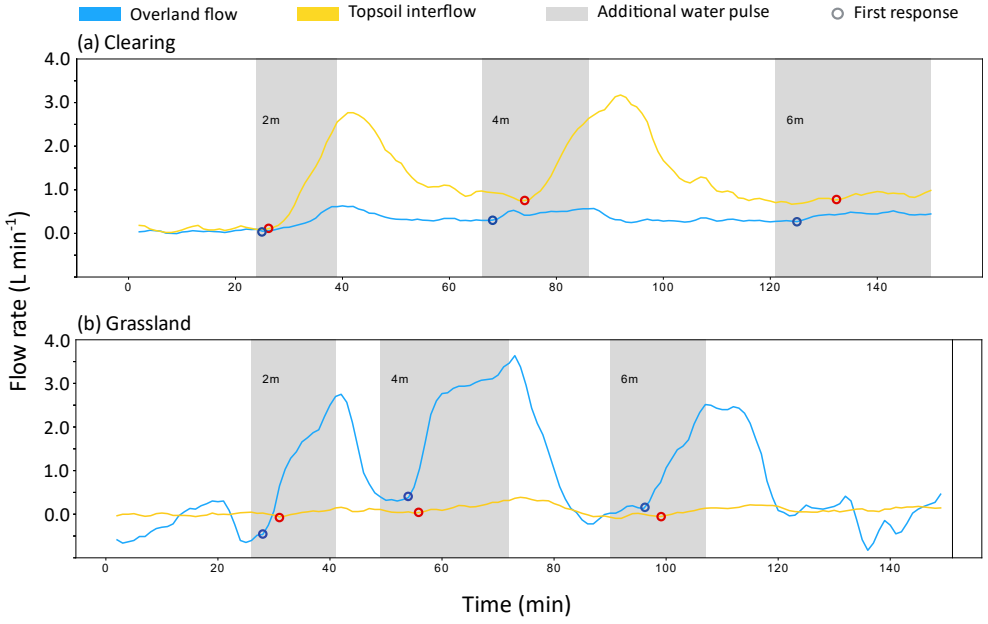

Figure 5: Time series for the increase in flow rates above the average steady state flow rate for OF (blue) and TIF (orange) during the water pulse experiments for the plot in the clearing (a) and the plot in the grassland (b). The times during which the additional water pulses were added are indicated with the gray shading. The time of the first increase in the flow rate in response to the water pulse (used for the calculation of the celerity) is indicated with a circle (blue for OF and red for TIF).

Table 4: Calculated celerity ± the estimated uncertainty for the water pulses applied at different distances from the trench for overland flow (OF) and topsoil interflow (TIF) for the plots in the clearing and the grassland, as well as the average value ± standard deviation for each plot. The uncertainty is based on an uncertainty of 2 minutes for the timing and 0.1 m for the distance.

Distance from trench (m)	Celerity ± uncertainty (m h^{-1})	
	OF	TIF
Clearing		
2	120 ± 240	40 ± 10
4	240 ±480	30 ± 11
6	90 ±45	33 ± 9
Average ± st. dev	150 ± 80	34 ± 5
Grassland		
2	60 ± 60	30 ± 7
4	60 ±19	48 ±8
6	72 ±20	41 ± 11
Average ± st. dev	64 ± 7	41 ±10

https://doi.org/10.5194/egusphere-2025-1677
Preprint. Discussion started: 15 April 2025

4.3. Tracer experiments

4.3.1. Breakthrough curves and particle velocities

The line tracers (NaCl and uranine) appeared within 3-13 minutes after application, depending on the distance from the trench that they were applied (Figure 6). The deuterium labelled water also appeared quickly in OF and TIF. It peaked after 36 minutes for OF and 112 minutes for TIF for the plot in the clearing and after 18 minutes for OF and 50 minutes for TIF for the plot in the grassland (Figure 6). The NaBr that was applied to the subsurface of the plot in the clearing mainly appeared in OF, arriving after 9 minutes for OF and after 27 minutes for TIF. For the plot in the grassland, NaBr concentrations remained below detection limits.

The calculated maximum particle velocities were generally higher for OF than TIF and were higher for the plot in the clearing than the plot in the grassland (Table 5). The average (± standard deviation) of the maximum particle velocities (calculated for the different tracers) for the plot in the clearing was 51 ± 14 m h^{-1} for OF and 30 ± 9 m h^{-1} for TIF. For the experiments on the grassland plot, the average of the maximum particle velocities was 24 ± 1 m h^{-1} for OF and 17 ± 6 m h^{-1} for TIF (Table 5).

https://doi.org/10.5194/egusphere-2025-1677
Preprint. Discussion started: 15 April 2025

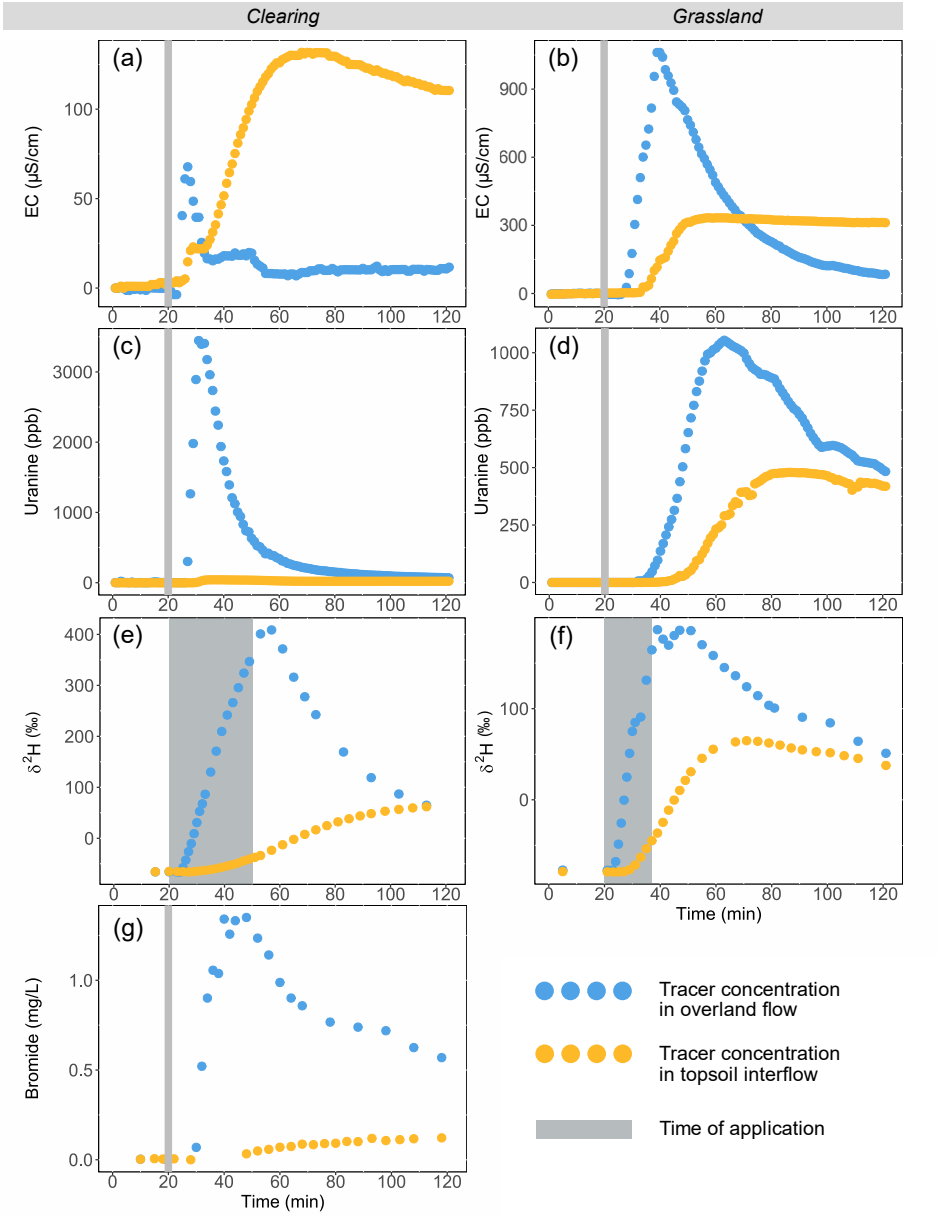

Figure 6: Breakthrough curves for the first lines of NaCl (EC minus background EC; first row) and uranine (second row), the deuterium labelled water added via the sprinklers (δ^2H; third row), and the NaBr applied to the subsurface (fourth row) for OF (blue) and TIF (orange) for the plot in the natural clearing (left column) and the plot in the grassland (right column). The bromide concentrations for the grassland plot remained below detection limit and are therefore not shown. Note that time 0 in panel a, c, e, and g correspond to minute 138 in Figure 4a, while time 0 in panels b, d, f corresponds to minute 50 in Figure 4b. The gray shaded areas indicate the time of the tracer applications. For the responses for the second line tracer applications, see Figure S1.

https://doi.org/10.5194/egusphere-2025-1677
Preprint. Discussion started: 15 April 2025

415

Table 5: Maximum particle velocities ± the estimated uncertainties for the tracers applied at different distances from the trench for overland flow (OF) and topsoil interflow (TIF) for the plots in the clearing and the grassland, as well as the average ± standard deviation for each plot. The uncertainty is based on an uncertainty of 2 minutes for the timing and 0.1 m for the distance. BDL stands for "below detection limit".

Location and tracer	Application distance trench (m)	Maximum particle velocity ± uncertainty (m h^{-1})	
		OF	TIF
Clearing			
NaCl 1	2.7	54 ± 38	27 ± 10
NaCl 2	6.0	72 ± 30	40 ± 10
Uranine 1	4.5	45 ± 16	30 ± 7
Uranine 2	7.5	35 ± 6	35 ± 6
NaBr	7.5	50 ± 12	17 ± 2
Average ± st. dev		51 ± 14	30 ± 9
Grassland			
NaCl	2.7	23 ± 8	13 ± 2
Uranine	4.5	25 ± 5	21 ± 4
NaBr	6.0	BDL	BDL
Average ± st. dev		24 ± 1	17 ± 6

420

4.3.2. Two-component mixing model

For the experiment in the clearing, the deuterium labelled water appeared after only 3 minutes in OF and after 11 minutes in TIF. A larger portion of the labelled water left the plot as OF than TIF, despite the flow rate being 35% lower for OF than TIF (Figure 7). The maximum fraction of labelled water in OF was 30% at 36 minutes after the
425 start of the application. The average fraction of labelled water in OF during the first 100 minutes of the experiment (including the 30-minute application period) was 15%. In contrast, the fraction of labelled water in TIF increased gradually, reaching a maximum of 8% at 112 minutes after the start of application o (i.e., 82 minutes after the end of the application).

In the grassland, the labelled water appeared in OF after 2 minutes and peaked at 10% 19 minutes after the start of
430 the application. Similar to the experiment in the clearing, the labelled water mainly left the plot as OF. The average contribution of the labelled water to OF during the first 100 minutes, however, was lower than for the clearing (7% vs 15%). The contribution of the labelled water to TIF was small, with a maximum of 5% at 51 minutes after the start of the application (i.e., 34 minutes after the end of the application) and an average of 4% for the first 100 minutes of the experiment (Figure 7). The response was, however, fast with the first arrival of the labelled water
435 after just 6 minutes.

https://doi.org/10.5194/egusphere-2025-1677
Preprint. Discussion started: 15 April 2025

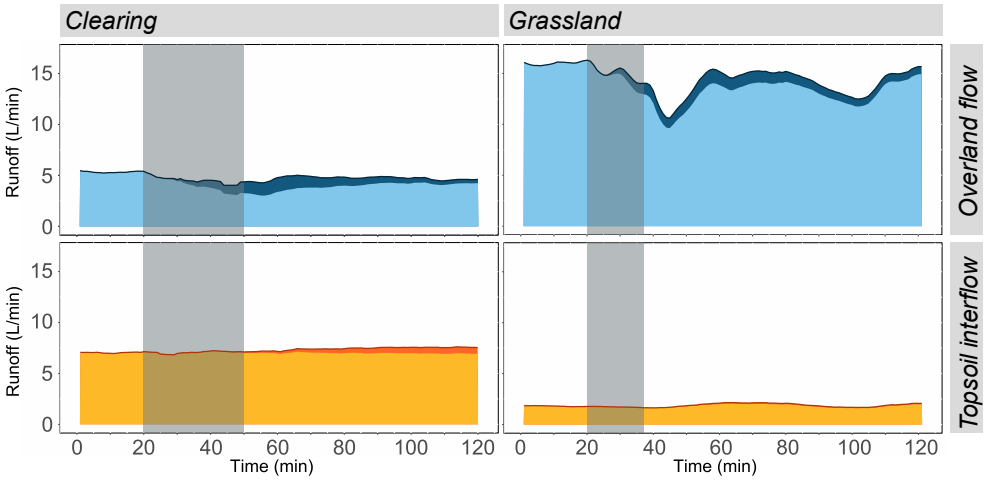

Figure 7: Overland flow (top row, blue) and topsoil interflow (bottom panel, orange) rates, with the contribution of the labelled water represented by the darker shades of blue and orange, respectively for the plot in the clearing (left) and the plot in the grassland (right). The grey shading indicates the time of the application of the labelled water. Note that time 0 in the figure for the clearing (left) corresponds to minute 138th minute in Figure 4a, and for the plot in the grassland (right) to minute 50 in Figure 4b.

4.3.3. Tracer recovery

For the plot in the clearing, most of the applied NaCl left the plot as TIF (Table 6; Figure 4), whereas most of the uranine that was applied only a few meters further upslope (Figure 3), left the plot as OF. The recovery of the NaBr, which was applied to the topsoil, was minimal after 100 minutes (<1% for both flow pathways). The recovery of uranine and NaCl for the grassland plot were much higher than for the plot in the clearing (14% vs 107% for NaCl and 27% vs 104% for uranine) and more similar for the two flow pathways (Table 6), despite the much higher flow rate for OF than TIF. The tracer recoveries exceeding 100% in the grassland are large attributed to the uncertainties in the flow measurements. The recovery of the labelled water after 100 minutes was more similar for the two plots but still twice as high for the plot in the grassland than the plot in the clearing: 12% for the clearing vs 24% for the grassland. After 24 hours, 39% of the labelled water was recovered for the plot in the clearing, with about one-third of the labelled water leaving the plot as OF and two-thirds as TIF (Table 6).

https://doi.org/10.5194/egusphere-2025-1677
Preprint. Discussion started: 15 April 2025

Table 6: Tracer recovery for the experiments on the plot in the clearing and the plot in the grassland. The second lines of NaCl and uranine were applied to the plot in the clearing 163 minutes after the application of the first line. Thus, tracer recovery after 100 and 163 minutes includes only the first tracer lines, while the recovery of NaCl and uranine after 24 hours includes both tracer lines. BDL stands for "below detection limit". Some of the tracer applied to the plot in the clearing likely left via an outflow on the side of the plot (see section 4.4). This will have reduced recovery of the tracers applied upslope from this outflow (NaCl 2, uranine 2, NaBr, and deuterium-labelled water).

Location and tracer	Tracer recovery (% applied mass)					
	After 100 minutes		After 163 minutes		After 24 hours	
	OF	TIF	OF	TIF	OF	TIF
Clearing						
NaCl	1	13	2	22	25	47
Uranine	25	2	26	3	17	3*
NaBr	<1	<1	<1	<1	1	<1
δ^2H	8	4	9	8	13	26
Grassland						
NaCl	94	13	No data			
Uranine	97	7				
NaBr	BDL	BDL				
δ^2H	22	2				

*Only for the first 385 minutes (6.4 hours) after application of first tracer line

4.4. OF Flowpath lengths

Most of the dye infiltrated into the soil after a short distance but there were a few longer flow pathways for both plots (Figure 8). The dye was observed to exfiltrate a short distance below the infiltration points (Figure 8), often from small pipes and mouse borrows. In the clearing, the dye flowed over the surface for 0 to 0.75 m (mean: 0.5 ± 0.8 m) before infiltrating. There was a longer flowpaths on the right side of the plots (when looking upslope) that was 3 m long (up to 5 m when including the water that exfiltrated; Figures 8 and 9). In the grassland, flow pathways were generally longer and more similar to each other, typically between 0.5 and 2 m (mean: 1.1 ± 0.3 m). The exfiltration points were also closer to the infiltration points than in the clearing and appeared to occur on parallel lines (Figure 8). When including the exfiltration points, the overall flowpath length was longer for the plot in the grassland (mean: 1.7 ± 0.5 m; Figure 9).

https://doi.org/10.5194/egusphere-2025-1677
Preprint. Discussion started: 15 April 2025

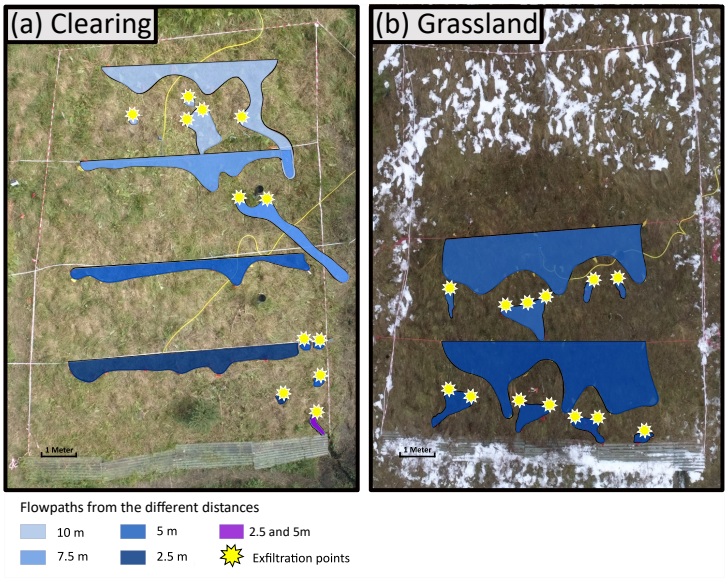

Figure 8: Drone images of the plot the clearing (a) and the grassland (b), with polygons indicating the OF pathways on the surface (blue shading, with different colors representing the results for the dye applications at different distances from the trench, and the exfiltration points where the dye stained OF re-emerged at the surface (yellow stars). The violet shading indicates the flow path observed for both the application at 2.5 m and at 5 m.

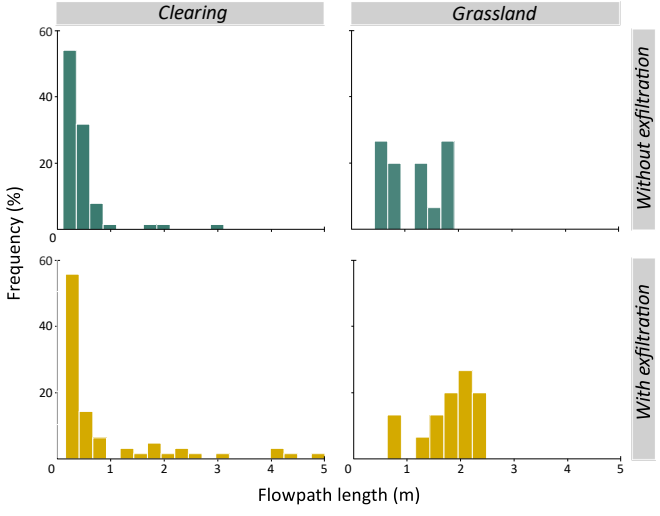

Figure 9: Frequency distribution of the distances that OF travelled over the surface before infiltrating into the soil (top row), and the total flow path length when including the OF path of the exfiltrating dye stained water (bottom) for the experiments in the clearing (left) and the grassland (right).

https://doi.org/10.5194/egusphere-2025-1677
Preprint. Discussion started: 15 April 2025

5. Discussion

5.1 Short OF flow pathways

The blue dye tracer experiments showed that (as expected) OF does not occur over the entire plots. Instead, the OF pathways were short and OF infiltrated within several meters. However, the experiments also highlighted the importance of exfiltration of OF after travelling only a short distance below the surface. Return flow (RF; Dunne, 1978) appeared on the surface 0.5 to 5 m after infiltration, and mostly created small ponds around the exfiltration points. Occasionally, the RF exfiltrated close to a depression or another exfiltration point, and the combined amount was enough to create a longer flow pathway. At both plots, the blue dye that exfiltrated still had an intense color, which suggests that it did not mix with a very large volume of soil water before exfiltration.

In the clearing the OF paths were mainly short (mean: ~ 0.5 m), which would be expected in a forested environment with high conductivity soils (cf. Gerke et al., 2015) but the microtopography also led to some longer flow pathways. This was mainly the case for the depressions that channelized OF on the upper part of the plot to the middle of the plot, creating an OF flow pathway up to 3 m long (Figure 8a). The exfiltration points were randomly distributed across the surface of the plot in the clearing. The ~4 cm diameter "pipe" for the relative long subsurface flow pathway (up to 4.5 m) from which water exfiltrated just above the bottom of the plot and OF gutter (Figure 8a) appeared to be a mouse burrow, and likely part of a network of macropores that provided almost all the OF collected in the gutter. Although other dye tracing studies for macropores (e.g., Mosley, 1979) have been criticised for creating unnatural boundary conditions, we don't think that pouring of the dye on the surface caused the flow through these preferential flow pathways as we observed that exfiltration from the main "pipe" delivered the majority of OF during natural rainfall events as well. Similar to the sprinkling experiments, these events also cause near saturated conditions. Pipes can reach up to tens of meters in some catchments (Jones, 2010, Wilson 2015) and can be major contributors to OF (called *pipe overland flow* by Putty and Prasad (2000)). Considering the runoff ratio for OF of ~ 20% for the plot in the clearing, it means that this macropore provided a considerable part of the total flow. Previous studies elsewhere (e.g., Tromp-van Meerveld and McDonnell, 2006; Uchida et al., 2003) have shown that single macropores can provide a very large portion of subsurface flow measured in a trench. The high celerity and velocity of OF and large amount of flow from this macropore (see also section 5.3.2) indicate that the network is quite shallow (i.e., near the surface), well connected, and that overland flow infiltrated quickly into it. If the network consists at least partly of mouse burrows, it is not surprising that it is very shallow because the water table is often located near the surface (Rinderer et al., 2024). Overall, these observations confirm those of previous studies that preferential flow via soil pipes and macropores is important for runoff generation in forested areas of the Swiss pre-Alps underlain by gleysols (Feyen et al., 1999; Weiler et al., 1998; Weiler and Naef, 2003).

In the grassland, the OF pathways were a bit longer than in the clearing and of a more similar length (~ 1 m), but also followed the microtopography. The exfiltration points were located closer to the infiltration points and were aligned across the plot. We attribute this to the microtopography caused by cow trampling, where OF infiltrates on the top of the "terraces" caused by the trampling (and subsequent solifluction) and exfiltrates at the bottom (see Figure 8b).

Few studies have observed OF pathways in-situ. Dye has been used commonly to observe flow pathways and macropores, but generally to visualize infiltration (Weiler and Flühler, 2004; Weiler and Naef, 2003) or lateral subsurface flow (Noguchi et al., 1999; Ehrhardt et al., 2022) and its connectivity (Anderson et al., 2009a). Only

https://doi.org/10.5194/egusphere-2025-1677
Preprint. Discussion started: 15 April 2025

very few studies have used tracers to observe overland flow in natural environments (Gerke et al., 2015; Maier et al., 2023). Nevertheless, the short OF pathways observed in this study agree with the general observation that OF pathways are short. For instance, Schneider et al. (2014) observed that dye applied to the surface on a 30° pre-Alpine grassland could flow 1 to 2 meters downslope from the application. Gerke et al. (2015) measured for a less vegetated forested slope flow paths up to 20 cm. In a dryland, OF flowpaths length were much longer, ranging between 1 to 6 m (Wolstenholme et al., 2020).

5.2 Tracer transport

The tracer experiments revealed the fast transport of solutes and the considerable interaction between OF and TIF, as the NaBr tracer applied to the subsurface of the clearing appeared after a short time in OF (Figure 6). As suggested by the dye tracer experiments (section 5.1), this indicates the exfiltration of soil water (i.e., return flow, RF). Furthermore, the peak concentration of the NaBr tracer was higher for OF than for TIF, which suggests that some of the NaBr reached preferential flow pathways and exfiltrated as RF next to the gutter, while the tracer that flowed through the subsurface mixed with a larger volume of water. However, the low recovery of NaBr suggests that most of the tracer remained in the subsurface (or left via the sides of the plot, or seeped into deeper soil layers). Feyen et al. (1999) showed that for a plot in a neighboring catchment that less than 0.5% of the stored soil water was mobilized during the event and that the majority of the soil does not contribute to flow in the subsurface. This could suggest that a large part of the subsurface applied tracer could still be stored in the soil. However, the fact that a significant portion of the tracers applied to the surface of the clearing left the plot during the full day of sprinkling suggests that a substantial amount of labelled water infiltrated into the soil matrix and was gradually released.

The heterogeneity of flow pathways, importance of infiltration of OF, transport through macropores and subsequent exfiltration as RF is highlighted by the recovery of the tracers that were applied to the surface of the clearing. The NaCl that was applied closest to the trench in the clearing was primarily recovered in TIF, suggesting predominantly infiltration of the tracer and subsurface transport. Contrary, the uranine applied 1.8 m further upslope was mostly recovered in OF (Figure 6). This suggests that this tracer infiltrated into the soil as well but also exfiltrated again after a short distance. In other words, the tracer applied further upslope reached a preferential flow network that provide RF, while the tracer applied further downslope did not and flowed through the subsurface. Again, this highlights the high spatial variation and heterogeneity in flow pathways.

The influence of macropores and soil pipes in facilitating the transport of water and tracer (see also section 5.1) was clearer for the plot in the clearing than the plot in the grassland. In the grassland, interactions between the flow pathways appeared less pronounced, as suggested by the predominant transport of the tracers in OF and much higher flow rate for OF than TIF (Figure 7). Furthermore, nearly all of the surface-applied line tracers were fully recovered within 100 minutes because less of it infiltrated into the soil than for the plot in the clearing. This difference can be related to differences in soil density and especially macroporosity. We observed a dense rooting system in the topsoil of the clearing but also found pieces of old buried wood deeper in the soil through (or along) which preferential flow might occur (Noguchi et al., 1999). In the grassland, the roots were finer and denser at the surface than the remainder of the topsoil, potentially limiting deeper infiltration and favoring biomat flow. However, the blue-dye experiments in the grassland still revealed the existence of exfiltration points (see Figure 8), which suggests that infiltration and exfiltration of OF takes place on the grassland as well. Furthermore, the recovery of the surface-applied tracers in TIF over the first 100-minutes was similar for both plots. This suggests

https://doi.org/10.5194/egusphere-2025-1677
Preprint. Discussion started: 15 April 2025

that although most of the water was transported as OF in the grassland, a similar amount of the tracers reached the trench via TIF as in the clearing.

The lack of any recovery of the NaBr tracer for the grassland plot might be related to the fewer number of macropores in the subsurface and overall slow flow through the subsurface (as also indicated by the low flow rates of TIF). Additionally, we might have applied too little water upslope of the tracer due to water supply limitations (see Figure 3) or the lack of NaBr recovery might be due to the short time of the experiment on the grassland plot (although it was still considerably longer than the time required for the NaBr to arrive in the trench and gutter in the clearing).

Although the main differences in the flow rates and tracer transport between the plot in the clearing and the grassland can be attributed to the differences in the amount of TIF and number and size of the preferential flow pathways, other factors differed as well (Table 1). The grassland plot has a steeper slope (18°) than the clearing (7°). Infiltration is generally less for steeper slopes (Essig et al., 2009; Morbidelli et al., 2013), which can explain the low amount of TIF for the grassland plot and low tracer recover in TIF. The bulk density (Table 1) was higher for the grassland than the clearing, which reflect the lower macroporosity and causes slower infiltration (Basset et al., 2023; Zhang et al., 2006). The higher bulk density may be the result of compaction due to cattle trampling (Hiltbrunner et al., 2012), less bioturbation in the grassland, or different rooting densities. The organic matter content near the surface (up to 15 cm) was also higher for the clearing, which may explain the higher macroporosity (cf. Franzluebbers, 2001; Kochiieru et al., 2022).

Furthermore, there were differences in the experimental setup (Figure 3; Table 2). The higher recovery of labelled water for the grassland plot may be due to the higher rainfall intensity for the experiment on the grassland plot (35 ± 13 vs 22 ± 2 mm h^{-1}). Higher intensity events can lead to more OF but may also lead to more preferential flow that can quickly transfer water and tracers through the topsoil. Feyen et al. (1999) did not measure any OF during lower intensity sprinkling experiments (8 mm h^{-1}) on a forested plot in a neighbouring catchment. Instead, the rainfall went primarily to deeper runoff and interflow through connected pores in the subsurface. Contrary, Weiler et al. (1999) conducted a high intensity sprinkling experiment (60 mm h^{-1}) on a forested plot in another nearby catchment and measured higher flow rates for OF than subsurface flow and high event water fractions (f_e) for both OF (90%) and subsurface flow (78%) (Weiler et al., 1999). However, measurements at 14 smaller plots by Gauthier et al. (2025) suggest that the precipitation thresholds for OF and TIF are similar and that the relative importance of OF to the total amount of near-surface flow (OF+TIF) increases with event size (i.e., total precipitation).

Additionally, the experiments were taken at different times of the growing season. As the experiment in the grassland was conducted at the end of the growing season, the vegetation was shorter and flattened by the snow that fell in the days preceding the experiments. This may have influenced the surface roughness and thus the OF dynamics (cf. Bond et al., 2020) and therefore the interaction between OF and subsurface flow pathways. We do not think that the snow cover itself affected the flow of the applied water as the initial testing of the sprinklers and the water applied to the plot to reach steady state flow conditions melted all the snow, and the soil temperatures were well above freezing (average 5.4 °C during the tracer experiments based on the temperature measurements by the soil moisture sensors).

https://doi.org/10.5194/egusphere-2025-1677
Preprint. Discussion started: 15 April 2025

5.3 High velocities and celerities

5.3.1. Velocities

The particle velocity (and celerity, see section 5.3.2) were high for both OF and TIF and both plots. The average (over all tracers) of the maximum particle velocity for OF was 51 m h^{-1} for the plot in the clearing and 24 m h^{-1} for the plot in the grassland. Few studies determined OF velocities for vegetated hillslopes but the values for the two plots in this study seem to be within the range of other studies, albeit on the lower side. For example, Holden et al. (2008) compared OF velocities on peatlands with different vegetation covers and bare surfaces using different flow rates (0.05-0.5 L s^{-1}). They reported a mean overland flow velocity of 104 m h^{-1} (range: 0.44-688 m h^{-1}). Bond et al. (2020) examined OF velocities on different grassland plots during different seasons in northern England by simulating a 18 mm h^{-1} rain event. They measured OF velocities between 93 and 149 m h^{-1}. The lower velocities in this study could be due to differences in water application (inflow from hoses instead of sprinklers) and the relatively high flow rates, leading to overland flow depths of up to 6 cm (Bond et al., 2020), which we did not observe. Furthermore, the plots in the previous studies were bounded and considerably smaller (0.5 m by 6 m (Holden et al., 2008) and 0.4 by 2.0 m (Bond et al., 2020)). Overland flow velocities might be higher on smaller, bounded plots due to limited infiltration opportunities, a reduced effect of microtopography, or edge effects. Additionally, overland flow velocities reported by Holden et al. (2008) include measurements from bare plots where flow velocities were about 5-10 times faster than for vegetated plots.

The average (over all tracers) of the maximum particle velocity for TIF was 30 m h^{-1} for the plot in the clearing and 17 m h^{-1} for the plot in the grassland. These velocities fall within the upper range of velocities reported for forest and grassland sites with preferential flow pathways (cf. Anderson et al., 2009b; Wienhöfer et al., 2009), although higher velocities have been reported for pipeflow and macropore flow (e.g., Graham et al., 2010; Mosley, 1979, 1982). For instance, Feyen et al., (1999) conducted tracer experiments on two 13 m^2 forested plots in a neighboring catchment with a sprinkling rate of ~ 8 mm h^{-1} and applied bromide as line tracer to the surface. The velocities during this experiment were 9 m h^{-1} for the site with muck humus and 0.5 m h^{-1} for the site with mor humus. The velocity of a salt tracer that was injected into the topsoil at 30 cm depth was 11 m h^{-1} for the muck humus site and 3 m h^{-1} for the mor humus site. These findings highlighted that fast flow through the topsoil via a network of conducting pores. We assume that the higher velocities reported in the present study are due to the considerably higher sprinkling rates that will have promoted flow through even larger macropores.

Weiler et al. (1998) conducted high-intensity (60-100 mm h^{-1}) sprinkling experiments in a near-by catchment on somewhat similar sized plots located in a grassland and a forest and reported higher flow velocities for the grassland (22-144 m h^{-1}) than the forest (5.4 m h^{-1}). The higher flow velocities in the grassland were attributed to macropores created by animals, which were larger in diameter compared to the denser but smaller pores formed by plant roots in the forest. For the plot in the clearing in this study, we observed several macropores created by animals, thus the plot is more comparable to the one in the grassland of Weiler et al. (1998) than their forested site.

5.3.2. Celerities

The average value of the celerities for OF (over all locations where we applied the water pulse) was 150 m h^{-1} for the plot in the clearing and 64 m h^{-1} for the plot in the grassland. In the clearing, we found a particularly high celerity for OF for the pulse at 4 m from the trench and gutter (240 m h^{-1}). After removing this outlier, the mean

https://doi.org/10.5194/egusphere-2025-1677
Preprint. Discussion started: 15 April 2025

celerity of OF in the clearing was still high (105 m h^{-1}) and almost twice as fast as for the grassland. The celerities for TIF were similar for the clearing (34 m h^{-1}) and the grassland (41 m h^{-1}).

The saturated and steady state conditions make it difficult to compare the celerities for this study to those in other studies. Furthermore, there are differences in the way that celerities are calculated. The celerities for TIF are lower than the initial hillslope celerities reported by Scaini et al., (2018) for natural events for a catchment in Luxembourg (90 ± 106 m h^{-1}) but are comparable to their integrated hillslope celerities (25 ± 34 m h^{-1}) for flow at the soil-bedrock interface, which is much deeper than the flow pathways studied here. The celerities are much higher than those reported by van Verseveld et al. (2017) (0.01-0.4 m h^{-1}), who estimated wetting front celerities during sprinkling experiments based on soil moisture, water level and soil matric potential measurements. However, the average sprinkling rate used by van Verseveld et al. (2017) was only 3-4 mm h^{-1} and the experiment was conducted on unsaturated soils.

As a result, of the high celerity for OF in the clearing, the difference in the celerity for OF and TIF was much larger for the clearing than the grassland. We hypothesize that the high celerity for OF in the clearing is due to flow through almost filled soil pipes that lead to return flow (RF) just above the trench and gutter (see also section 5.1). The high sprinkling intensities and near saturated conditions at steady state conditions during the experiment, likely contributed to the high celerities (and also velocities). However, these near saturated conditions are not uncommon in the Studibach catchment (see also Gauthier et al., 2025; Rinderer et al., 2014, 2019), as reflected by the return period of the applied rainfall intensity and the relatively short wetting period required to reach saturation/steady state conditions during the experiments.

5.3.3 Comparison of velocities and celerities

Previous studies compared the velocity and celerity by using the kinematic ratio (α_k being the ratio of celerity divided by velocity; Rasmussen 2000). For our study, α_k for OF ranged between 2 and 3. For TIF, this ratio depended on the location. For the plot in the grassland, the celerity was also two to three times higher than the particle velocity but for the plot in the clearing, the celerity and particle velocity were nearly identical. The latter is similar to the values reported by Scaini et al. (2017) (α_k :1.02-1.06) for subsurface flow in permeable soils (Dystric Endoskeletic Cambisol) above a slate bedrock in a forested catchment in Luxembourg. Contrary to this study and the study by Scaini et al. (2017), van Verseveld et al. (2017) and Torres et al. (1998) found much higher values of α_k for high permeability colluvial soils (3-20 and 15, respectively). For flow through discrete pore networks (rather than more diffusive flow through the soil matrix) α_k tends to one (Hrachowitz et al., (2016). The results thus provide further evidence of the importance of preferential flow, especially in the clearing, as also highlighted by the blue dye experiments (section 5.1) and the tracer recovery (section 5.2).

6. Conclusions

We used rainfall simulation and tracer experiments on two 8 m wide plots in a steep humid pre-Alpine catchment with low permeability gleysols to better understand overland flow (OF) and lateral flow through the topsoil (topsoil interflow, TIF). For the plot in a natural clearing in the open forest, the applied water infiltrated quickly and flowed through preferential flow networks (i.e., macropores) downslope. Part of this water resurfaced as return flow a few meters after infiltrating, but most flowed through the topsoil as TIF. For the plot in the grassland, most of the applied water left the plot as OF and less water was transported as TIF, likely due to the lower macroporosity of

https://doi.org/10.5194/egusphere-2025-1677
Preprint. Discussion started: 15 April 2025

the soil. Tracer transport during steady state conditions was fast, with velocities ranging between 17 to 51 mm h^{-1}. The celerity was 2-3 times higher than the velocity, except for TIF in the clearing for which it was similar as the velocity. Together, these findings highlight the importance of preferential flow for the fast response of OF and TIF, and likely also the fast response of streams in this and other pre-Alpine catchments with gleysols.

Data availability

Data can be provided by the corresponding authors upon request and will be uploaded to the Envidat data repository (www.envidat.ch).

Author contributions

AL, VAG and IvM conceptualized the study and planned the experiments and data collection. AL and VAG collected the data, analyzed the data and wrote the manuscript draft; AL, VAG, and IvM reviewed and edited the manuscript. IvM supervised the project. The order of the two first authors was determined with a coin flip (with a 2 CHF coin from 1973 on the blue square at Irchel campus on 3.4.2025).

Competing interests

The authors declare that they have no conflict of interest.

Acknowledgements

We thank our colleagues from the H2K group at the Department of Geography at the University of Zurich, Sandro Wiesendanger, Anja Ehrensperger, Elena Köpfli, and Amaury Berjaoui and Louise Fuchs for their help in setting up the plots and the experiments. We thank Barbara Herbstritt (University of Freiburg) for the isotope analyses and Björn Studer (ETH Zurich) for the bromide analyses. We thank the Oberallmeindkorporation Schwyz (OAK), the Department of Environment of the Canton of Schwyz, and the municipality Alpthal for their cooperation. This research was conducted as part of the TopFlow: (in)visible water flows near the surface project funded by the Swiss National Science Foundation (Grant 197194).

References

Anderson, A. E., Weiler, M., Alila, Y., and Hudson, R. O.: Dye staining and excavation of a lateral preferential flow network, Hydrol. Earth Syst. Sci., 2009a.

Anderson, A. E., Weiler, M., Alila, Y., and Hudson, R. O.: Subsurface flow velocities in a hillslope with lateral preferential flow, Water Resources Research, 45, https://doi.org/10.1029/2008WR007121, 2009b.

Anderson, S. P., Dietrich, W. E., Montgomery, D. R., Torres, R., Conrad, M. E., and Loague, K.: Subsurface flow paths in a steep, unchanneled catchment, Water Resources Research, 33, 2637–2653, https://doi.org/10.1029/97WR02595, 1997.

https://doi.org/10.5194/egusphere-2025-1677
Preprint. Discussion started: 15 April 2025

Bachmair, S. and Weiler, M.: Hillslope characteristics as controls of subsurface flow variability, Hydrology and Earth System Sciences, 16, 3699–3715, https://doi.org/10.5194/hess-16-3699-2012, 2012.

Basset, C., Abou Najm, M., Ghezzehei, T., Hao, X., and Daccache, A.: How does soil structure affect water infiltration? A meta-data systematic review, Soil and Tillage Research, 226, 105577, https://doi.org/10.1016/j.still.2022.105577, 2023.

Bazemore, D. E., Eshleman, K. N., and Hollenbeck, K. J.: The role of soil water in stormflow generation in a forested headwater catchment: synthesis of natural tracer and hydrometric evidence, Journal of Hydrology, 162, 47–75, https://doi.org/10.1016/0022-1694(94)90004-3, 1994.

Bond, S., Kirkby, M. J., Johnston, J., Crowle, A., and Holden, J.: Seasonal vegetation and management influence overland flow velocity and roughness in upland grasslands, Hydrological Processes, 34, 3777–3791, https://doi.org/10.1002/hyp.13842, 2020.

Brown, V. A., McDonnell, J. J., Burns, D. A., and Kendall, C.: The role of event water, a rapid shallow flow component, and catchment size in summer stormflow, Journal of Hydrology, 217, 171–190, https://doi.org/10.1016/S0022-1694(98)00247-9, 1999.

Buttle, J. M. and McDonald, D. J.: Coupled vertical and lateral preferential flow on a forested slope, Water Resources Research, 38, 18–1, https://doi.org/10.1029/2001WR000773, 2002.

Dunne, T.: Field Studies of Hillslope Flow Processes The dynamics surface processes in response to the declining Dead Sea level View project, in: Hillslope Hydrology, edited by: Kirkby, M. J., John Wiley & Sons, Chichester, UK, 1978.

Ehrhardt, A., Berger, K., Filipović, V., Wöhling, T., Vogel, H., and Gerke, H. H.: Tracing lateral subsurface flow in layered soils by undisturbed monolith sampling, targeted laboratory experiments, and model-based analysis, Vadose Zone Journal, 21, e20206, https://doi.org/10.1002/vzj2.20206, 2022.

Essig, E. T., Corradini, C., Morbidelli, R., and Govindaraju, R. S.: Infiltration and deep flow over sloping surfaces: Comparison of numerical and experimental results, Journal of Hydrology, 374, 30–42, https://doi.org/10.1016/j.jhydrol.2009.05.017, 2009.

Feyen, H., Wunderli, H., Wydler, H., and Papritz, A.: A tracer experiment to study flow paths of water in a forest soil, Journal of Hydrology, 225, https://doi.org/10.1016/S0022-1694(99)00159-6, 1999.

Franzluebbers, A. J.: Water infiltration and soil structure related to organic matter and its stratification with depth, 2001.

Freer, J., McDonnell, J., Beven, K. J., Brammer, D., Burns, D., Hooper, R. P., and Kendal, C.: Hydrological processes—Letters. Topographic controls on subsurface storm flow at the hillslope scale for two hydrologically distinct small catchmetns, Hydrological Processes, 11, 1347–1352, https://doi.org/10.1002/(SICI)1099-1085(199707)11:9<1347::AID-HYP592>3.0.CO;2-R, 1997.

Freer, J., McDonnell, J. J., Beven, K. J., Peters, N. E., Burns, D. A., Hooper, R. P., Aulenbach, B., and Kendall, C.: The role of bedrock topography on subsurface storm flow, Water Resources Research, 38, 5-1-5–16, https://doi.org/10.1029/2001wr000872, 2002.

Gauthier, V. A., Leuteritz, A., and van Meerveld, I.: When and where does near-surface runoff occur in a pre-Alpine headwater catchment?, Hydrology and Earth System Sciences Discussions, 2025, 1–25, https://doi.org/10.5194/hess-2024-398, 2025.

Gerke, K. M., Sidle, R. C., and Mallants, D.: Preferential flow mechanisms identified from staining experiments in forested hillslopes, Hydrological Processes, 29, 4562–4578, https://doi.org/10.1002/hyp.10468, 2015.

Graham, C. B., Woods, R. A., and McDonnell, J. J.: Hillslope threshold response to rainfall: (1) A field based forensic approach, Journal of Hydrology, 393, 65–76, https://doi.org/10.1016/j.jhydrol.2009.12.015, 2010.

https://doi.org/10.5194/egusphere-2025-1677
Preprint. Discussion started: 15 April 2025

Hagedorn, F., Schleppi, P., Waldner, P., and Flühler, H.: Export of dissolved organic carbon and nitrogen from Gleysol dominated catchments - The significance of water flow paths, Biogeochemistry, 50, https://doi.org/10.1023/A:1006398105953, 2000.

Hallema, D. W., Moussa, R., Sun, G., and McNulty, S. G.: Surface storm flow prediction on hillslopes based on topography and hydrologic connectivity, Ecol Process, 5, 13, https://doi.org/10.1186/s13717-016-0057-1, 2016.

Hiltbrunner, D., Schulze, S., Hagedorn, F., Schmidt, M. W. I., and Zimmmermann, S.: Cattle trampling alters soil properties and changes soil microbial communities in a Swiss sub-alpine pasture, Geoderma, 170, 369–377, https://doi.org/10.1016/j.geoderma.2011.11.026, 2012.

Holden, J., Kirkby, M. J., Lane, S. N., Milledge, D. G., Brookes, C. J., Holden, V., and McDonald, A. T.: Overland flow velocity and roughness properties in peatlands, Water Resources Research, 44, https://doi.org/10.1029/2007WR006052, 2008.

Hrachowitz, M., Benettin, P., van Breukelen, B. M., Fovet, O., Howden, N. J. K., Ruiz, L., van der Velde, Y., and Wade, A. J.: Transit times—the link between hydrology and water quality at the catchment scale, WIREs Water, 3, 629–657, https://doi.org/10.1002/wat2.1155, 2016.

Jackson, C. R., Du, E., Klaus, J., Griffiths, N. A., Bitew, M., and McDonnell, J. J.: Interactions among hydraulic conductivity distributions, subsurface topography, and transport thresholds revealed by a multitracer hillslope irrigation experiment, Water Resources Research, 52, 6186–6206, https://doi.org/10.1002/2015WR018364, 2016.

Jones, J. A. A.: Soil piping and catchment response, Hydrological Processes, 24, 1548–1566, https://doi.org/10.1002/hyp.7634, 2010.

Kienzler, P. M. and Naef, F.: Subsurface storm flow formation at different hillslopes and implications for the "old water paradox," Hydrological Processes, 22, 104–116, https://doi.org/10.1002/hyp.6687, 2008.

Klaus, J., Zehe, E., Elsner, M., Külls, C., and McDonnell, J. J.: Macropore flow of old water revisited: experimental insights from a tile-drained hillslope, Hydrol. Earth Syst. Sci., 17, 103–118, https://doi.org/10.5194/hess-17-103-2013, 2013.

Kochiieru, M., Lamorski, K., Feizienė, D., Feiza, V., Šlepetienė, A., and Volungevičius, J.: Land use and soil types affect macropore network, organic carbon and nutrient retention, Lithuania, Geoderma Regional, 28, e00473, https://doi.org/10.1016/j.geodrs.2021.e00473, 2022.

Maier, F. and van Meerveld, I.: Long-Term Changes in Runoff Generation Mechanisms for Two Proglacial Areas in the Swiss Alps I: Overland Flow, Water Resources Research, 57, https://doi.org/10.1029/2021WR030221, 2021.

Maier, F., Lustenberger, F., and Van Meerveld, I.: Assessment of plot-scale sediment transport on young moraines in the Swiss Alps using a fluorescent sand tracer, Hydrol. Earth Syst. Sci., 27, 4609–4635, https://doi.org/10.5194/hess-27-4609-2023, 2023.

McDonnell, J. J.: A Rationale for Old Water Discharge Through Macropores in a Steep, Humid Catchment, Water Resources Research, 26, 2821–2832, https://doi.org/10.1029/WR026i011p02821, 1990.

McDonnell, J. J. and Beven, K.: Debates—The future of hydrological sciences: A (common) path forward? A call to action aimed at understanding velocities, celerities and residence time distributions of the headwater hydrograph, Water Resources Research, 50, 5342–5350, https://doi.org/10.1002/2013WR015141, 2014.

McGuire, K. J. and McDonnell, J. J.: Hydrological connectivity of hillslopes and streams: Characteristic time scales and nonlinearities, Water Resources Research, 46, 2010WR009341, https://doi.org/10.1029/2010WR009341, 2010.

van Meerveld, H. J., Baird, E. J., and Floyd, W. C.: Controls on sediment production from an unpaved resource road in a Pacific maritime watershed, Water Resources Research, 50, 4803–4820, https://doi.org/10.1002/2013WR014605, 2014.

https://doi.org/10.5194/egusphere-2025-1677
Preprint. Discussion started: 15 April 2025

van Meerveld, H. J., Fischer, B. M. C., Rinderer, M., Stähli, M., and Seibert, J.: Runoff generation in a pre-alpine catchment: A discussion between a tracer and a shallow groundwater hydrologist, Geographical Research Letters, 44, https://doi.org/10.18172/cig.3349, 2018.

Meißl, G., Geitner, C., Batliner, A., Klebinder, K., Kohl, B., and Markart, G.: Brixenbach research catchment: Quantification of runoff process proportions in a small Alpine catchment depending on soil moisture states and precipitation characteristics, Hydrological Processes, 35, https://doi.org/10.1002/hyp.14186, 2021.

Meißl, G., Klebinder, K., Zieher, T., Lechner, V., Kohl, B., and Markart, G.: Influence of antecedent soil moisture content and land use on the surface runoff response to heavy rainfall simulation experiments investigated in Alpine catchments, Heliyon, 9, e18597, https://doi.org/10.1016/j.heliyon.2023.e18597, 2023.

Mohn, J., Schürmann, A., Hagedorn, F., Schleppi, P., and Bachofen, R.: Increased rates of denitrification in nitrogen-treated forest soils, Forest Ecology and Management, 137, 113–119, https://doi.org/10.1016/S0378-1127(99)00320-5, 2000.

Monger, F., Bond, S., Spracklen, D. V., and Kirkby, M. J.: Overland flow velocity and soil properties in established semi-natural woodland and wood pasture in an upland catchment, Hydrological Processes, 36, https://doi.org/10.1002/hyp.14567, 2022.

Montgomery, D. R., Dietrich, W. E., Torres, R., Anderson, S. P., Heffner, J. T., and Loague, K.: Hydrologic response of a steep, unchanneled valley to natural and applied rainfall, Water Resources Research, 33, 91–109, https://doi.org/10.1029/96WR02985, 1997.

Morbidelli, R., Corradini, C., Saltalippi, C., Flammini, A., and Govindaraju, R. S.: The role of slope on the overland flow production, WIT Transactions on Ecology and the Environment, 172, 63–71, https://doi.org/10.2495/RBM130061, 2013.

Mosley, M. P.: Streamflow generation in a forested watershed, New Zealand, Water Resources Research, 15, 1979.

Mosley, M. P.: Subsurface flow velocities through selected forest soils, South Island, New Zealand, Journal of Hydrology, 55, 65–92, https://doi.org/10.1016/0022-1694(82)90121-4, 1982.

Noguchi, S., Tsuboyama, Y., Sidle, R. C., and Hosoda, I.: Morphological Characteristics of Macropores and the Distribution of Preferential Flow Pathways in a Forested Slope Segment, Soil Science Soc of Amer J, 63, 1413–1423, https://doi.org/10.2136/sssaj1999.6351413x, 1999.

Putty, M. R. Y. and Prasad, R.: Runoff processes in headwater catchments—an experimental study in Western Ghats, South India, Journal of Hydrology, 235, 63–71, https://doi.org/10.1016/S0022-1694(00)00262-6, 2000.

Rasmussen, T. C., Baldwin, R. H., Dowd, J. F., and Williams, A. G.: Tracer vs. Pressure Wave Velocities through Unsaturated Saprolite, Soil Science Soc of Amer J, 64, 75–85, https://doi.org/10.2136/sssaj2000.64175x, 2000.

Rinderer, M., Van Meerveld, H. J., and Seibert, J.: Topographic controls on shallow groundwater levels in a steep, prealpine catchment: When are the TWI assumptions valid?, Water Resources Research, 50, https://doi.org/10.1002/2013WR015009, 2014.

Rinderer, M., van Meerveld, I., Stähli, M., and Seibert, J.: Is groundwater response timing in a pre-alpine catchment controlled more by topography or by rainfall?, Hydrological Processes, 30, 1036–1051, https://doi.org/10.1002/hyp.10634, 2016.

Rinderer, M., van Meerveld, H. J., and McGlynn, B. L.: From Points to Patterns: Using Groundwater Time Series Clustering to Investigate Subsurface Hydrological Connectivity and Runoff Source Area Dynamics, Water Resources Research, 55, 5784–5806, https://doi.org/10.1029/2018WR023886, 2019.

Saco, P. M. and Kumar, P.: Kinematic dispersion effects of hillslope velocities, Water Resources Research, 40, 2003WR002024, https://doi.org/10.1029/2003WR002024, 2004.

Scaini, A., Audebert, M., Hissler, C., Fenicia, F., Gourdol, L., Pfister, L., and Beven, K. J.: Velocity and celerity dynamics at plot scale inferred from artificial tracing experiments and time-lapse ERT, Journal of Hydrology, 546, 28–43, https://doi.org/10.1016/j.jhydrol.2016.12.035, 2017.

https://doi.org/10.5194/egusphere-2025-1677
Preprint. Discussion started: 15 April 2025

Scaini, A., Hissler, C., Fenicia, F., Juilleret, J., Iffly, J. F., Pfister, L., and Beven, K.: Hillslope response to sprinkling and natural rainfall using velocity and celerity estimates in a slate-bedrock catchment, Journal of Hydrology, 558, 366–379, https://doi.org/10.1016/j.jhydrol.2017.12.011, 2018.

Scherrer, S., Naef, F., Faeh, A. O., and Cordery, I.: Formation of runoff at the hillslope scale during intense precipitation, Hydrol. Earth Syst. Sci, 11, 907–922, 2007.

Schleppi, P., Muller, N., Feyen, H., Papritz, A., Bucher, J. B., and Flühler, H.: Nitrogen budgets of two small experimental forested catchments at Alptal, Switzerland, Forest Ecology and Management, 101, 177–185, https://doi.org/10.1016/S0378-1127(97)00134-5, 1998.

Schleppi, P., Hagedorn, F., and Providoli, I.: Nitrate Leaching From a Mountain Forest Ecosystem with Gleysols Subjected to Experimentally Increased N Deposition, Water, Air, and soil Pollution, 453–467, 2004.

Schneider, P., Pool, S., Strouhal, L., and Seibert, J.: True colors-experimental identification of hydrological processes at a hillslope prone to slide, Hydrology and Earth System Sciences, 18, 875–892, https://doi.org/10.5194/hess-18-875-2014, 2014.

Shannon, J., Liu, F., Van Grinsven, M., Kolka, R., and Pypker, T.: Magnitude, consequences and correction of temperature-derived errors for absolute pressure transducers under common monitoring scenarios, Hydrological Processes, 36, https://doi.org/10.1002/hyp.14457, 2022.

Sidle, R. C., Tsuboyama, Y., Noguchi, S., Hosoda, I., Fujieda, M., and Shimizu, T.: Stormflow generation in steep forested headwaters: a linked hydrogeomorphic paradigm, Hydrol. Process., 14, 369–385, https://doi.org/10.1002/(SICI)1099-1085(20000228)14:3<369::AID-HYP943>3.0.CO;2-P, 2000.

Sidle, R. C., Noguchi, S., Tsuboyama, Y., and Laursen, K.: A conceptual model of preferential flow systems in forested hillslopes: evidence of self-organization, Hydrological Processes, 15, 1675–1692, https://doi.org/10.1002/hyp.233, 2001.

Sidle, R. C., Hirano, T., Gomi, T., and Terajima, T.: Hortonian overland flow from Japanese forest plantations - An aberration, the real thing, or something in between?, Hydrological Processes, 21, 3237–3247, https://doi.org/10.1002/hyp.6876, 2007.

Stähli, M. and Gustafsson, D.: Long-term investigations of the snow cover in a subalpine semi-forested catchment, Hydrological Processes, 20, 411–428, https://doi.org/10.1002/hyp.6058, 2006.

Stähli, M., Seibert, J., Kirchner, J. W., von Freyberg, J., and van Meerveld, I.: Hydrological trends and the evolution of catchment research in the Alptal valley, central Switzerland, Hydrological Processes, 35, https://doi.org/10.1002/hyp.14113, 2021.

Tani, M.: Runoff generation processes estimated from hydrological observations on a steep forested hillslope with a thin soil layer, Journal of Hydrology, 200, 84–109, https://doi.org/10.1016/S0022-1694(97)00018-8, 1997.

Torres, R., Dietrich, W. E., Montgomery, D. R., Anderson, S. P., and Loague, K.: Unsaturated zone processes and the hydrologic response of a steep, unchanneled catchment, Water Resources Research, 34, 1865–1879, https://doi.org/10.1029/98WR01140, 1998.

Tromp-van Meerveld, H. J. and McDonnell, J. J.: Threshold relations in subsurface stormflow: 1. A 147-storm analysis of the Panola hillslope, Water Resources Research, 42, 2004WR003778, https://doi.org/10.1029/2004WR003778, 2006.

Tromp-Van Meerveld, H. J. and McDonnell, J. J.: Threshold relations in subsurface stormflow: 2. The fill and spill hypothesis, Water Resources Research, 42, https://doi.org/10.1029/2004WR003800, 2006.

Tsuboyama, Y., Sidle, R. C., Noguchi, S., and Hosoda, I.: Flow and solute transport through the soil matrix and macropores of a hillslope segment, Water Resources Research, 30, 879–890, https://doi.org/10.1029/93WR03245, 1994.

Uchida, T., Asano, Y., Ohte, N., and Mizuyama, T.: Seepage area and rate of bedrock groundwater discharge at a granitic unchanneled hillslope, Water Resources Research, 39, https://doi.org/10.1029/2002WR001298, 2003.

https://doi.org/10.5194/egusphere-2025-1677
Preprint. Discussion started: 15 April 2025

Uchida, T., Tromp-van Meerveld, I., and McDonnell, J. J.: The role of lateral pipe flow in hillslope runoff response: an intercomparison of non-linear hillslope response, Journal of Hydrology, 311, 117–133, https://doi.org/10.1016/j.jhydrol.2005.01.012, 2005.

van Verseveld, W. J., Barnard, H. R., Graham, C. B., McDonnell, J. J., Brooks, J. R., and Weiler, M.: A sprinkling experiment to quantify celerity–velocity differences at the hillslope scale, Hydrology and Earth System Sciences, 21, 5891–5910, https://doi.org/10.5194/hess-21-5891-2017, 2017.

Vlček, L., Falátková, K., and Schneider, P.: Identification of runoff formation with two dyes in a mid-latitude mountain headwater, Hydrol. Earth Syst. Sci., 21, 3025–3040, https://doi.org/10.5194/hess-21-3025-2017, 2017.

Wadman, M.: Spatial variability of infiltration in a pre-alpine catchment, unpublished Master's thesis, Wageningen University, 2023.

Weiler, M. and Flühler, H.: Inferring flow types from dye patterns in macroporous soils, Geoderma, 120, 137–153, https://doi.org/10.1016/j.geoderma.2003.08.014, 2004.

Weiler, M. and Naef, F.: An experimental tracer study of the role of macropores in infiltration in grassland soils, Hydrological Processes, 17, 477–493, https://doi.org/10.1002/hyp.1136, 2003.

Weiler, M., Naef, F., and Leibundgut, C.: Study of runoff generation on hillslopes using tracer experiments and a physically based numerical hillslope model, IAHS Publications, 353–360, 1998.

Weiler, M., Scherrer, S. C., Naef, F., and Burlando, P.: Hydrograph separation of runoff components based on measuring hydraulic state variables, tracer experiments, and weighting methods, IAHS-AISH publication, 249–255, 1999.

Weiler, M., McDonnell, J. J., Tromp-van Meerveld, I., and Uchida, T.: Subsurface Stormflow, in: Encyclopedia of Hydrological Sciences, https://doi.org/10.1002/0470848944.hsa119, 2006.

Wienhöfer, J., Germer, K., Lindenmaier, F., Färber, A., and Zehe, E.: Applied tracers for the observation of subsurface stormflow at the hillslope scale, Hydrology and Earth System Sciences, 13, 1145–1161, https://doi.org/10.5194/hess-13-1145-2009, 2009.

Wolstenholme, J. M., Smith, M. W., Baird, A. J., and Sim, T. G.: A new approach for measuring surface hydrological connectivity, Hydrological Processes, 34, 538–552, https://doi.org/10.1002/hyp.13602, 2020.

Woods, R. and Rowe, L.: The Changing Spatial Variability of Subsurface Flow Across a Hillside, Journal of Hydrology (NZ), 35, 51–86, 1996.

Zhang, S., Grip, H., and Lövdahl, L.: Effect of soil compaction on hydraulic properties of two loess soils in China, Soil and Tillage Research, 90, 117–125, https://doi.org/10.1016/j.still.2005.08.012, 2006.